Molecular Microbiology (2016) 99(5), 909–924 ■
doi: 10.1111/mmi.13275
First published online 9 December 2015

A phosphorylation code of the *Aspergillus nidulans* global regulator VelvetA (VeA) determines specific functions

Stefan Rauscher,[1] Sylvia Pacher,[1] Maren Hedtke,[1] Olaf Kniemeyer[2] and Reinhard Fischer[1,*]
[1]*Institute for Applied Biosciences, Department of Microbiology, Karlsruhe Institute of Technology, Hertzstrasse 16, D-76187 Karlsruhe, Germany.*
[2]*Leibniz Institute for Natural Product Research and Infection Biology, Hans-Knöll-Institute (HKI), Adolf-Reichwein-Str. 23, 07745 Jena, Germany.*

Summary

The velvet protein VeA is a global fungal regulator for morphogenetic pathways as well as for the control of secondary metabolism. It is found exclusively in filamentous fungi, where it fulfills conserved, but also unique functions in different species. The involvement of VeA in various morphogenetic and metabolic pathways is probably due to spatially and timely controlled specific protein–protein interactions with other regulators such as phytochrome (FphA) or velvet-like proteins (VelB). Here we present evidence that *Aspergillus nidulans* VeA is a multi-phosphorylated protein and hypothesize that at least four specific amino acids (T167, T170, S183 and Y254) undergo reversible phosphorylation to trigger development and sterigmatocystin biosynthesis. Double mutation of T167 to valine and T170 to glutamic acid exerted the largest effects with regards to sexual development and *veA* gene expression. In comparison with wild-type VeA, which shuttles out of the nuclei after illumination this VeA variant showed stronger nuclear accumulation than the wild type, independent of the light conditions. The interaction between VeA and VelB or FphA, respectively, was affected in the T167V-T170E mutant. Our results suggest complex regulation of the phosphorylation status of the VeA protein.

Introduction

Environmental conditions and internal cues determine microbial growth and development. This requires a large number of sensing systems, which are often located at the cytoplasmic membrane, and subsequent cytoplasmic signal transduction cascades. In the case of eukaryotes, signals often have to be transmitted into the nucleus and therefore signal cascades usually consist of several proteins. Such complex signaling cascades, in addition, allow the integration of different signals into a single biological response. One possibility for such integration is that a key protein interacts with proteins from different pathways at certain times or at certain subcellular locations. A beautiful example is the fungal protein VeA, which is important for several morphogenetic processes, but also controls secondary metabolism through a number of different protein partners (Bayram and Braus, 2012).

VeA is unique to filamentous fungi and contains a so-called velvet domain, typical for all proteins of the velvet protein family (Ahmed *et al.*, 2013; Park *et al.*, 2014). Other members of this family in *Aspergillus nidulans* are VelB, VelC and VosA that play a role in sexual development, spore viability and spore maturation (Bayram *et al.*, 2008; Bayram and Braus, 2012; Park *et al.*, 2012; 2014; Ahmed *et al.*, 2013). The founding member, *veA*, was first described after a mutagenesis screening in 1965 (Käfer, 1965). Whereas wild-type *A. nidulans* develops mainly asexually in light and sexually in the dark (Clutterbuck, 1977; Timberlake, 1990) mutation of *veA* (veA1) leads to a shift from sexual to asexual development in the dark. The mutation is very convenient because *A. nidulans* can be cultivated in dark incubators to generate asexual spores and study asexual development. Hence, the mutation was introduced into most of the laboratory strains used worldwide (Adams *et al.*, 1998). The identification of the corresponding gene by mutant complementation was almost 40 years later and revealed the *veA1* mutation as a point mutation in the first ATG resulting in a truncated protein with altered localization (Kim *et al.*, 2002). Whereas wild-type VeA is mainly localized in the cytoplasm in the light, and shuttles into the nucleus in the dark, the truncated VeA1 protein remains mainly cytoplasmic also in the dark (Stinnett *et al.*, 2007).

After the original discovery in *A. nidulans*, VeA has been studied in a number of different fungi. In the food contaminating fungi *Aspergillus parasiticus* and *Aspergillus flavus* the role of VeA homologs were described as key proteins for aflatoxin production (Calvo *et al.*, 2004; Duran *et al.*, 2007; Amaike and Keller, 2009; Calvo and Cary, 2015).

Accepted 10 November, 2015. *For correspondence. E-mail reinhard.fischer@KIT.edu; Tel. (+49) 721 608 44630; Fax (+49) 721 608 44509. Homepage: www.iab.kit.edu/microbio.

Just recently, distorted conidiophores and curved hyphae were reported as a result of the deletion of the *veA* gene in the industrially important *Aspergillus niger* (Wang *et al*., 2015). In other fungi with relevance for industrial applications, such as *Acremonium chrysogenum* (Dreyer *et al*., 2007) and *Penicillium chrysogenum*, *PcvelA* is essential for penicillin production (Hoff *et al*., 2010). In the human pathogenic fungus *Histoplasma capsulatum*, velvet was shown to be required for the temperature-mediated switch from hyphal to yeast-like growth and is therefore necessary for pathogenicity, but also for spore viability (Webster and Sil, 2008; Beyhan *et al*., 2013). In *Aspergillus fumigatus* VeA controls conidiation, gliotoxin formation and protease activity (Dhingra *et al*., 2012). In the plant pathogenic fungus *Botrytis cinerea*, VeA is important for pathogenicity and sclerotia formation (Schumacher *et al*., 2015). Likewise, VeA was also characterized in other plant-pathogenic fungi, such as *Fusarium verticilloides* (Li *et al*., 2006; Myung *et al*., 2009), *Fusarium fujikuroi* (Wiemann *et al*., 2010), *Magnaporthe oryzae* (Kim *et al*., 2014) and *Ustilago maydis* (Karakkat *et al*., 2013). The large number of studies illustrates the relevance of VeA in fungal biology and its role as important regulator.

One question is of course how VeA can be involved in such a variety of different processes and one of the answers is that VeA is able to interact with several other proteins and is thus interlinked with different pathways. *A. nidulans* VeA interacts with the potential methyltransferase LaeA in a heterotrimeric complex together with the velvet-like protein, VelB (Bayram *et al*., 2008). Therefore, VeA plays a central role as an activator of secondary metabolite production like sterigmatocystin (ST) and penicillin (Kato *et al*., 2003). But there are also reports of VeA acting as a repressor of orsillinic acid biosynthesis. This effect involves changes in histone acetylation (Bok *et al*., 2013). In a Δ*veA* mutant, *gcnE* (encoding a histone acetyltransferase) expression is induced. These observations fit to recent results where differential gene expression of over 26% of the genome was observed in a *veA*-deletion strain as compared with wild type (40% of the 498 secondary metabolite genes) (Lind *et al*., 2015). Further interaction partners of VeA are the phytochrome FphA, that comprises an active kinase domain and is necessary for the expression of light induced genes (Blumenstein *et al*., 2005; Brandt *et al*., 2008; Purschwitz *et al*., 2008; Hedtke *et al*., 2015), the methyl transferases VipC, VapB (Sarikaya-Bayram *et al*., 2014) and LlmF (Palmer *et al*., 2013). Velvet-interacting protein A, VipA, is yet another protein of interest, but its exact function still needs to be determined (Calvo, 2008).

As for the mode of action of VeA, besides being an interaction partner for many proteins, it is important to consider the structure of the protein. VeA contains a bipartite nuclear localization signal (NLS), a nuclear export signal (NES), two PEST (rich in: proline (P), glutamic acid (E), serine (S) and threonine (T)) motifs and a so-called *velvet* domain. PEST domains are typical for proteins with a high turnover rate and often become phosphorylated (Rechsteiner, 1990; Rechsteiner and Rogers, 1996). The velvet domain is found in all velvet-like proteins and the one from VosA was crystallized recently (Ahmed *et al*., 2013). The 3-D structure revealed analogies to the RH domain (rel homologous domain) that can be found in eukaryotic transcription factors like NF-κB. Further investigation indeed showed DNA-binding capabilities of the velvet domain (Ahmed *et al*., 2013). Thus, VeA could have the potential for direct gene control and is probably a key to understanding differential gene expression in many filamentous fungi. Proteins with RH domains actually change target gene transcription dependent on their phosphorylation status (Anrather *et al*., 2005). Hence, phosphorylation could also be crucial in VeA signaling. Likewise, FphA is a kinase and interacts with VeA (Brandt *et al*., 2008; Purschwitz *et al*., 2008). However, even if FphA phosphorylates VeA, deletion of *fphA* did not completely abolish phosphorylation (Purschwitz *et al*., 2009). Another kinase phosphorylating VeA was discovered with the MAP kinase MpkB, a Fus3 homolog of *Saccharomyces cerevisiae* (Bayram *et al*., 2012). Deletion of *mpkB* showed a complete loss of sexual development whereas overexpression resulted in induction of cleistothecia (Jun *et al*., 2011). The signal input starts at the membrane and is transported via MpkB to the nucleus. It was suggested that this phosphorylation may affect the interaction of VeA with VelB (Bayram *et al*., 2012).

To further characterize the phosphorylation status of VeA and to start deciphering the role(s) of posttranslational modification(s), we determined four phosphorylation sites in VeA by peptide fingerprinting. Subsequent analysis of the role of the phosphorylation sites *in vivo* via site-directed mutagenesis revealed functions of VeA phosphorylation in ST production, development and *veA*-gene transcription. A combination of dephosphorylated threonine 167 and phosphorylated threonine 170 resulted in a partial *veA*-deletion phenotype and altered localization of VeA and its interaction with VelB and FphA.

Results

Identification of VeA phosphorylation sites

VeA is a protein with multiple functions through potential DNA-binding activity and several protein-interacting partners. There is good evidence that the VeA protein undergoes phosphorylation and one kinase with VeA as target was already identified (Purschwitz *et al*., 2009; Bayram *et al*., 2012). As VeA contains a PEST domain within the C-terminal region and these domains are typical targets

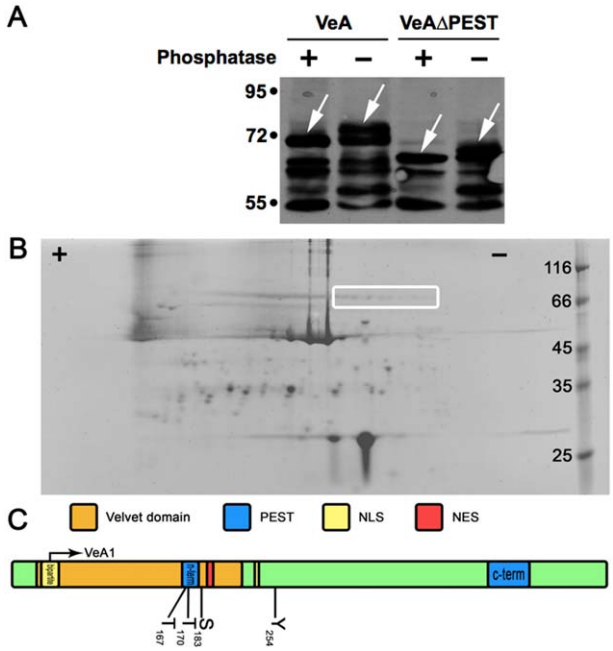

Fig. 1. VeA is a phosphorylated protein.
A. *Aspergillus nidulans* cultures were shaken in minimal medium containing 2% threonine and 0.2% glucose for 24 h at 37°C. 50 μg crude extract of SSM51 (*alcA(p)::3xHA::veA*) were immediately isolated and treated with or without (control) NEB λ-phosphatase for 1 h at 30°C and then loaded onto a 7.5% SDS gel. To exclude phosphorylation exclusively due to the C-terminal PEST domain, a deletion strain SSM52 (*alcA(p)::3xHA::veA*ΔPEST) was used for the same procedure.
B. VeA was precipitated with HA agarose and run on a 2-D gel. Anode (+) and cathode (–) are indicated by symbols. White box marked spots highlighted are full-length VeA variants on the ruthenium stained gel.
C. MALDI-TOF analysis of the highlighted spots from the 2-D gel showed four amino acids with potential phosphorylation. The velvet domains including the phosphorylation sites are depicted as well as the start codon used in the *veA1* mutant.

for phosphorylation, it was likely that VeA phosphorylation occurs there. To test if VeA phosphorylation also occurs outside the C-terminal PEST domain, the VeA protein and a VeA protein lacking this PEST domain were analyzed by Western blotting (Fig. 1A). VeA is a rather unstable protein and thus several degradation products were detected besides the 67 kDa and 60 kDa full-length HA–VeA fusion proteins. When crude cell extracts were treated with a λ-phosphatase, a shift of the upper bands was observed, suggesting loss of phosphate residues upon treatment (Fig. 1A). Because the shift was observed in VeA and VeAΔPEST, phosphorylation probably also occurs outside the PEST domain. This was also obvious in 2-D gels, in which several protein spots with the same molecular mass, but different isoelectric points occurred (Fig. 1B). VeA protein spots were confirmed by Western blot analysis of the 2-D gel using anti-HA antibodies (data not shown). These spots were analyzed by mass spectrometry (MS/MS) after tryptic digest (32% of the protein sequence was covered by the peptides). The analysis confirmed the identity of the spots as VeA and revealed three different peptides. Sequence inspection of the corresponding peptides suggested that threonine 167 and 170, serine 183 and tyrosine 254 can undergo phosphorylation (Fig. 1C). Unfortunately, we were yet unable to resolve the peptides of the C-terminal part of VeA. Therefore, we concentrated in the following on the functional analysis of the four potentially phosphorylated amino acids.

Using iTasser a 3-D model – based on the VosA velvet domain crystal structure – was generated to illustrate the location of amino acids T167, T170, S183 and Y254 within the protein structure. All phosphorylation sites appear to be accessible from the surface, and S183 and Y254 are located close to a potential protein interaction site (Fig. S1A) (Ahmed *et al.*, 2013). To check whether these residues are located within structural domains, the protein was analyzed with ePESTfind, which revealed another weak PEST domain in the N-terminal region as part of the velvet domain (Rechsteiner and Rogers, 1996; Bayram and Braus, 2012). The threshold in this analysis was set to 4.5 instead of the normal value 5. Interestingly T167 and T170 are situated in the N-terminal PEST domain. Sequence comparison of *A. nidulans* VeA with 30 VeA proteins from various species revealed that the phosphorylation sites are phylogenetically not conserved (Fig. S1B). Whereas the velvet domain is highly conserved, the regions with the phosphorylated amino acids, are quite variable. However, even if e.g. T170 appears to be present in *Aspergillus fumigatus*, *Aspergillus clavatus* and *Schwartziella fischeri*, in other fungi it is not conserved, but a threonine appears in the vicinity of this position.

VeA phosphorylation sites influence light-dependent development

After the identification of the four phosphorylated amino acids in VeA, we aimed at understanding their physiological significance. To this end, first a *veA*-deletion strain was generated by transformation of a *ptrA*-deletion cassette fused to a left-border fragment, LB (1.5 kbp upstream) and a right-border fragment, RB (1.5 kbp downstream) of the *veA* locus into *A. nidulans* SSR48 (Fig. S2). Next, a series of modified VeA versions was created and each construct used for *in locus* complementation of the Δ*veA*-deletion strain SSR56 (Fig. S3). Each amino acid was exchanged with a structurally comparable amino acid that resembles a silenced phosphorylation site (valine, alanine or phenylalanine instead of threonine, serine and tyrosine) or mimics constitutive phosphorylation with a negative charge (glutamic acid) (Fig. S4). Investigation of the colony growth speed revealed slower growth of the

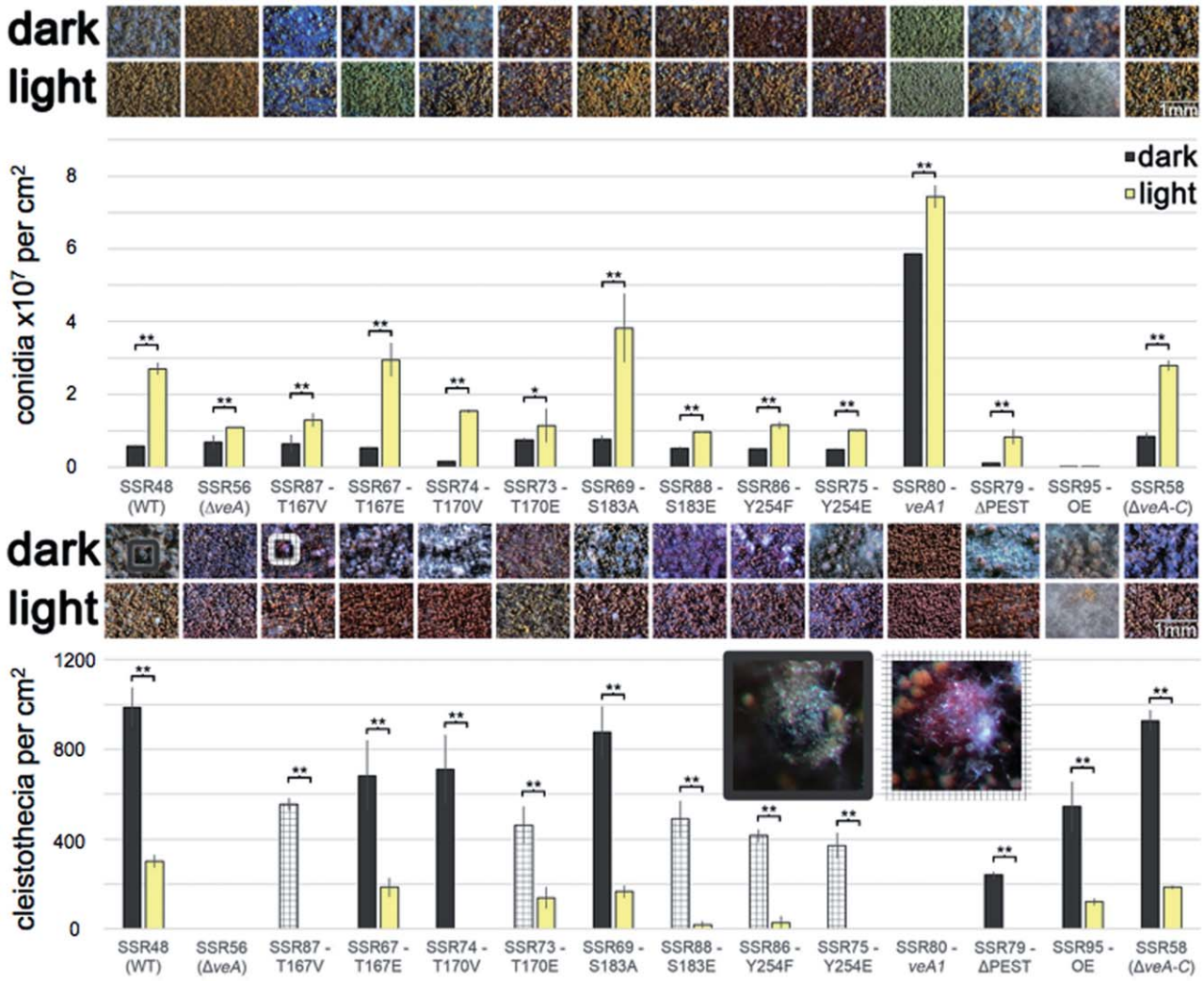

Fig. 2. Light induction of asexual development and cleistothecia maturation is activated by the same phosphorylation status of VeA. Different *veA* mutants were grown for 24 h in darkness at 37°C and subsequently illuminated for 48 h (light) or kept in darkness for the same time (dark) to investigate asexual development. Each strain and condition was done in triple replicates and spores were counted after incubation. For sexual development strains have been grown for 24 h in darkness at 37°C and afterwards constantly illuminated for 96 h in white light or kept in the dark. From each strain three independent samples were used to count the amount of cleistothecia from a defined area. Mutants that produced immature cleistothecia (magnification) at the time of investigation are indicated with a checkered pattern. Microscopic pictures were taken at the time of investigation. Error bars indicate the standard deviation and ** shows a *P*-value ≤ 0.01, * ≤ 0.05.

mutants *ΔveA*, *veA1* and T170V compared with the wild type (Fig. S5). In the following phenotypic analysis of light-dependent development a *veA1* mutant, a variant without the C-terminal PEST domain and a *veA* overexpression mutant (*h2B(p)::veA*) were included (Fig. 2). All strains were grown for 48 h (asexual) and 96 h (sexual) on agar plates in the dark or in light (7 J m^{-2}) and the number of conidiospores and the number of cleistothecia was determined. The wild type showed light-dependent conidiation, and the *veA1* mutant sporulated better than the wild type especially under dark conditions. The *veA*-deletion strain was affected in light stimulation. Overexpression caused a strong reduction of conidiation under all conditions. This strain produced more aerial mycelium and therefore appeared fluffy-like. The lack of the PEST domain caused a similar phenotype, although conidiation was still light sensitive. Strong light induction, like in wild type, was only observed in the mutants T167E, T170V, S183A. This suggests that T167 should be phosphorylated and T170 and S183 should be dephosphorylated in wild type to achieve light induction of conidiation. When the strains were analyzed for cleistothecia production, the same three amino acids turned out to be required for wild type-like formation and maturation of cleistothecia. The other strains were often delayed in their development. When compared at the same time, they only produced

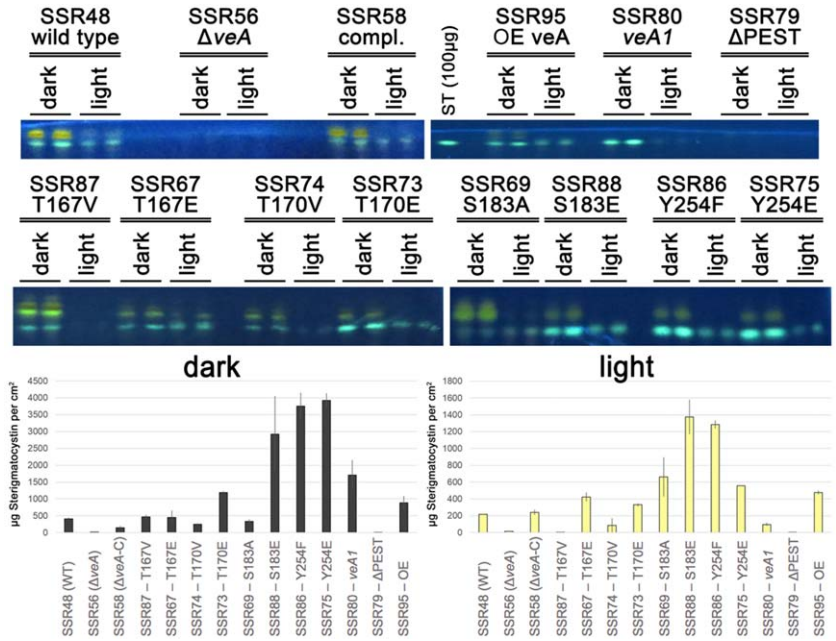

Fig. 3. S183E and Y254F mutants show induced ST production in light and dark. Strains were grown for 24 h in dark to achieve competence and afterwards incubated for additional 48 h at 37°C on MM containing 2% glucose subjected to white light or kept in the dark. A defined amount of agar was cut from the plates for ST purification. Thin-layer chromatography was performed with toluol : ethylacetate : acetic acid (80:10:10) running buffer. After treatment with $AlCl_3$ the plates were exposed to 365 nm UV light for detection of the bright blue ST band. 100 µg ST standard (Sigma-Aldrich) was loaded for each run. Band intensity was determined with ImageJ and normalized to the standard on each plate. Error bars indicate the standard deviation.
This figure is available in colour online at wileyonlinelibrary.com.

reddish structures and not the typical black cleistothecia. These reddish structures did not produce viable ascospores (data not shown). Further incubation at RT for a total of 5 weeks resulted in mature cleistothecia with strongly reddish-colored nursing cells (Fig. S6).

The phosphorylation status of serine S183 and tyrosine Y254 is important for ST production

To investigate the influence of VeA phosphorylation sites on the production of ST, all mutants were analyzed after 3 d of growth in the dark or 1 d in the dark and subsequent 2 d of white light illumination (7 J m^{-2}) at 37°C. Because ST production is influenced by many environmental parameters besides light, it was important to standardize the growth conditions (exact amounts of media, same batch of media). Sampling and ST analysis was done with two biological and two technical replicates. ST was analyzed by thin-layer chromatography and the amounts quantified by ImageJ (Fig. 3). The wild type produced 250% more ST in the dark compared with the illuminated samples whereas the *ΔveA*-deletion and the ΔPEST mutant produced no detectable ST. Most of the mutants behaved like the wild type with minor alterations. Interesting were the very high amounts of ST in the S183E, Y254F and Y254E (600–800% of the WT) mutants in darkness that also produced more ST after illumination. ST amounts after illumination were highest in the S183E and Y254F (650% to the WT) mutants whereas the S183A and Y254E mutants were still higher compared with the wild type (300%). The strongest opposing effect was observed at S183 in darkness where the silencing mutant S183A produced the same amounts of ST as the wild type, but the phosphorylation-mimicking mutant S183E showed 600% induction. A comparable regulation was observed in light. With regards to modifications of Y254, there was no different regulation between the two mutants Y254F and Y254E in darkness, but in the illuminated samples. The strain with the tyrosine mutation Y254F showed higher ST production than the Y254E mutant. Further, the T167V mutant resulted in loss of ST production after illumination and no difference in darkness, whereas the T167E mutant showed almost no inhibition after light treatment. The T170E mutant showed an increase of 250% ST production compared with the wild type in darkness, but only a slight increase compared with wild type in light. Taken together the phosphorylation status of S183 and Y254 influence ST production in *A. nidulans*, but light still represses ST production.

The expression of veA *depends on the phosphorylation status of T167 and T170*

After studying the developmental and metabolic phenotypic changes caused by interfering with the phosphorylation status of VeA, we aimed at understanding the molecular effects because of the modifications in the VeA protein. The function of VeA depends on its correct expression, but is also dependent on the correct subcellular distribution (Stinnett *et al.*, 2007; Kim *et al.*, 2009). In order to test whether any of the VeA modifications had an impact on VeA itself, *veA* expression was analyzed in wild

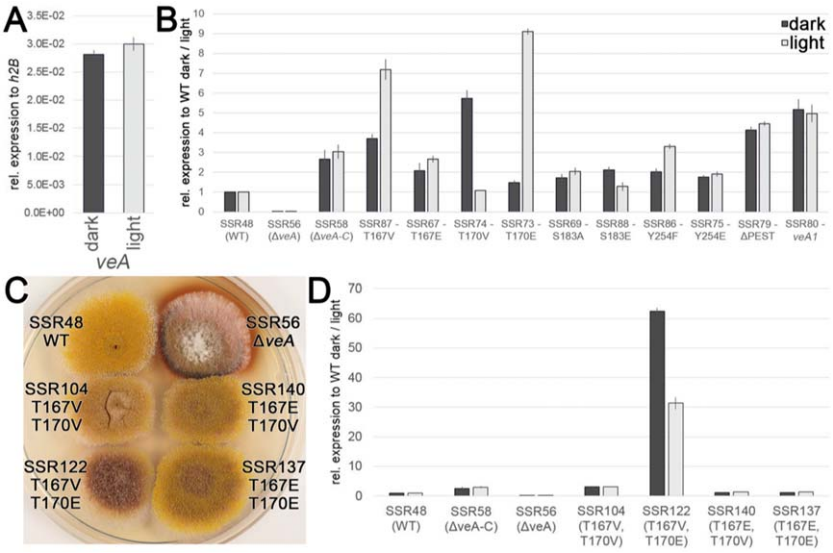

Fig. 4. The double-mutant T167V-T170E induces strong *veA*-gene expression and shows a colony phenotype.
A. Mutants were grown for 18 h at 37°C in darkness and afterwards either exposed to white light for 30 min or kept in the dark. RNA was isolated after the described treatment. Quantitative RT PCR was performed to determine *veA* expression level relative to *h2B*. Relative expression of wild-type *veA* did not change after illumination.
B. Expressions of the *veA* mutants were normalized to the wild-type expression in dark and light.
C. Strains carrying the double mutations at T167 and T170 were used to complement the *veA* deletion strain (SSR56). Colonies are shown after 4 d growth on MM (2% glucose) at 37°C.
D. Mutants were treated as in A and used for qRT-PCR to determine *veA* expression levels. Error bars represent the standard error.

type and the different mutants. It was reported that *veA* gene expression was induced after 14 h of growth under white light (Kim *et al.*, 2009). Here we show that *veA* expression is not yet altered after 30 min of illumination with white light (0.15 J m^{-2}) suggesting that *veA* gene expression is only affected by long-term illumination (Fig. 4A). To investigate if *veA* expression depends on the phosphorylation sites described earlier, the expression levels of *veA* were determined in darkness and after 30 min of white-light treatment (Fig. 4B). The mutants *ΔPEST* and *veA1* were elevated fivefold relative to the wild type independent of light. The mutants T167E, S183A, S183E, Y254F and Y254E did not appear to have different *veA*-expression levels relative to wild type and the re-complemented strain. The strongest change in *veA* expression was observed in the mutants T167V, T170V and T170E where the expression was increased. Whereas the strain with VeA T167V and T170E showed an increase of seven- to ninefold only after illumination, the T170V mutant possessed a sixfold induction only if kept in darkness. To further examine the roles of T167 and T170, double mutants that carried mutations of both amino acids in all four possible combinations were created. Colonies of these strains represented wild-type phenotype except for the T167V-T170E mutant that appeared rather like a *ΔveA*-deletion strain (Fig. 4C). Surprisingly, only the T167V-T170E mutant showed a very strong increase in *veA* expression, which was stronger in the dark than in light (Fig. 4D). The mutants T167E-T170E, T167E-T170V and T167V-T170V did not show any distinct increase compared with wild type. The VeA protein level was not determined because already in wild type, intact VeA is difficult to detect (Fig. 1). VeA undergoes quick protein turnover and thus many degradation products appear and the ratio between intact and degraded VeA varies. Because the *veA* transcript levels were already changed in the different mutant strains, differences in the protein level and correlations with the phenotypes would be very difficult to interpret. In addition, different phosphorylations could also affect protein stability and yet add another degree of complexity.

Mutant T167V-T170E partially phenocopies veA *deletion*

To investigate phenotypic effects of the double mutants, we analyzed ST production and sexual development. For the T167E-T170E and T167E-T170V mutants the only change in ST production was a decrease to 20% of the wild-type level after illumination (Fig. 5A). Whereas the T167V-T170V mutant almost lost ST production independent of light treatment, the T167V-T170E mutant showed no alteration after illumination and even an induction in darkness compared with wild type. At the same time the T167V-T170E mutant showed the appearance of a novel secondary metabolite after illumination, visible as a brownish fluorescence directly above the blue ST signal. Interestingly, the T167V-T170E mutant showed no production of fruiting bodies or nest-like structures similar to the *ΔveA*-deletion mutant (Fig. 5B). The strains T167E-T170E, T167V-T170V and T167E-T170V produced again reddish structures as reported earlier (Fig. 2).

VeA T167V-T170E mutant results in constitutive nuclear accumulation of the protein and fails to interact with VelB and FphA

Next, we analyzed the subcellular distribution of VeA and the T167V-T170E VeA variant. The full-length proteins were N-terminally fused to mCitrine and the constructs were used for *in locus* complementation of the *ΔveA*

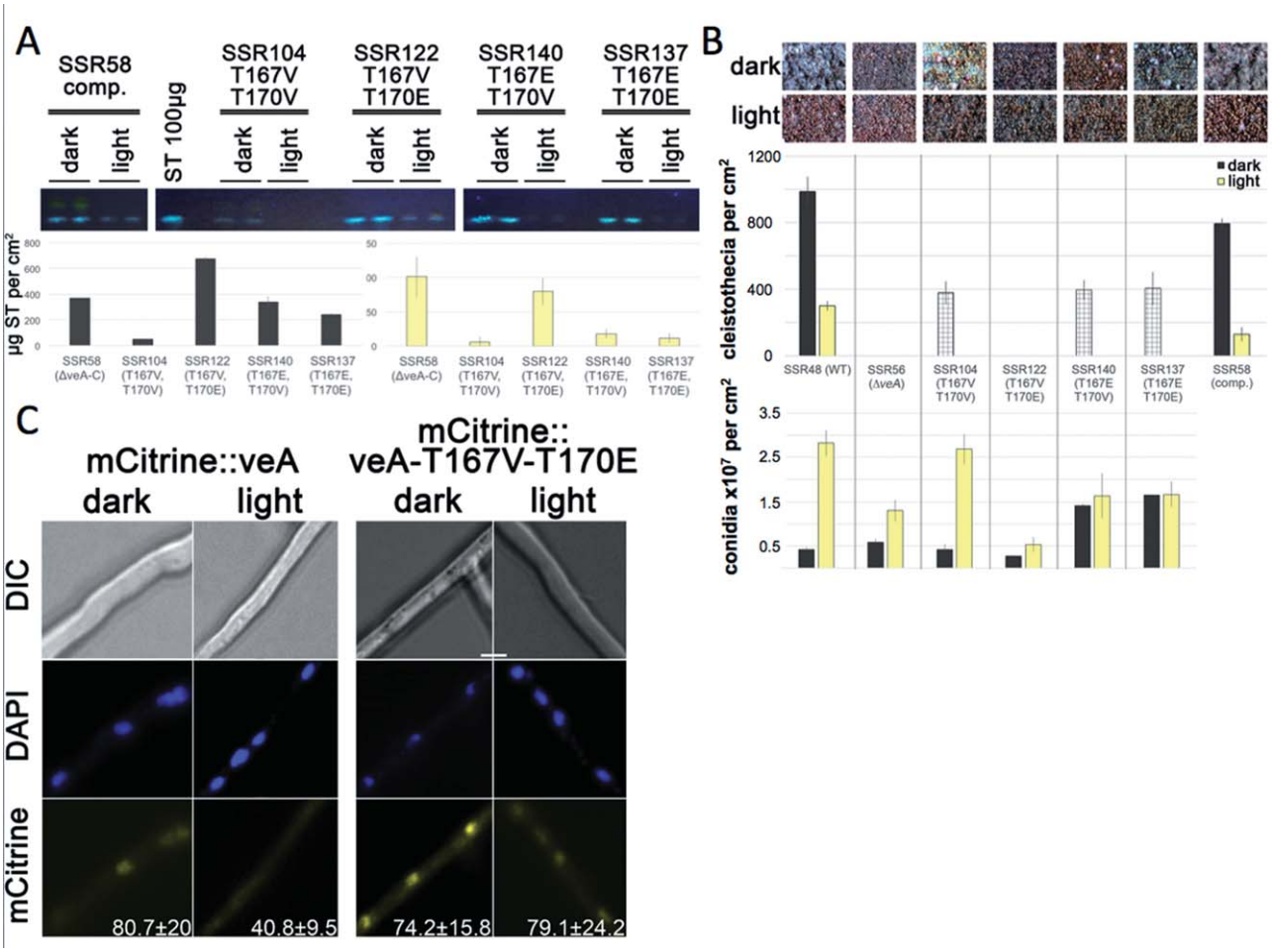

Fig. 5. The T167V-T170E mutant partially phenocopies *veA*-deletion and localizes predominantly in the nucleus.
A. Strains were grown for 24 h in darkness and subsequently exposed to white light for additional 48 h or kept in the dark. ST was isolated and analyzed with thin-layer chromatography and toluol : ethylacetate : acetic acid (80:10:10) running buffer.
B. The production of sexual structures was analyzed by growing the mutants for 24 h in darkness and afterwards shifted to white light or kept in the dark for additional 96 h on MM at 37°C. Quantification was performed in triple replicates from a specific area of each sample. Checkered columns indicate slowly maturing cleistothecia. Error bars in (A) and (B) represent the standard deviation.
C. Microscopic pictures of the T167V-T170E mutant and the wild type were gained by N-terminal fusion of the fluorescent protein mCitrine under the natural promoter and in locus recombination. The strains were grown overnight at 24°C on MM with 2% glucose in constant dark or white light and afterwards used for microscopy. Values indicate the percentage of fluorescence signals in the nucleus and standard deviation of at least six microscopic pictures from three independent experiments.

mutation. In the light, VeA localized mainly to the cytoplasm and shuttles into nuclei in the dark (Fig. 5C; Stinnett *et al.*, 2007). In contrast the T167V-T170E mutant revealed stronger nuclear localization even in the light. As the T167V-T170E mutant shows impaired sexual development, ST production and increased *veA* gene expression we looked into the interaction with VelB, another protein of the velvet protein family that interacts with VeA and shows comparable effects when lost (Bayram *et al.*, 2008). CoIP analysis with N-terminal GFP tagged VeA, or the T167V, T170E double mutant and HA-tagged VelB were performed and showed a loss of the interaction between the double-mutant protein and VelB (Fig. 6A). To confirm this, bimolecular fluorescence complementation (BiFC) assays were performed. VelB was fused to the N-terminal half of YFP while VeA and the T167V-T170E mutant were fused to the C-terminal part. Interaction of VelB and VeA was observed mainly within the nuclei as previously described (Bayram *et al.*, 2008), whereas there was no signal detected for the T167V-T170E mutant and VelB (Fig. 6B).

Additionally, interaction of the T167V-T170E double mutant protein with FphA was examined via BiFC. VeA and FphA interact in nuclei (Purschwitz *et al.*, 2009). However, the T167V-T170E mutation led only to weak cytosplasmic signals, clearly excluding the nuclei (Fig. 6B).

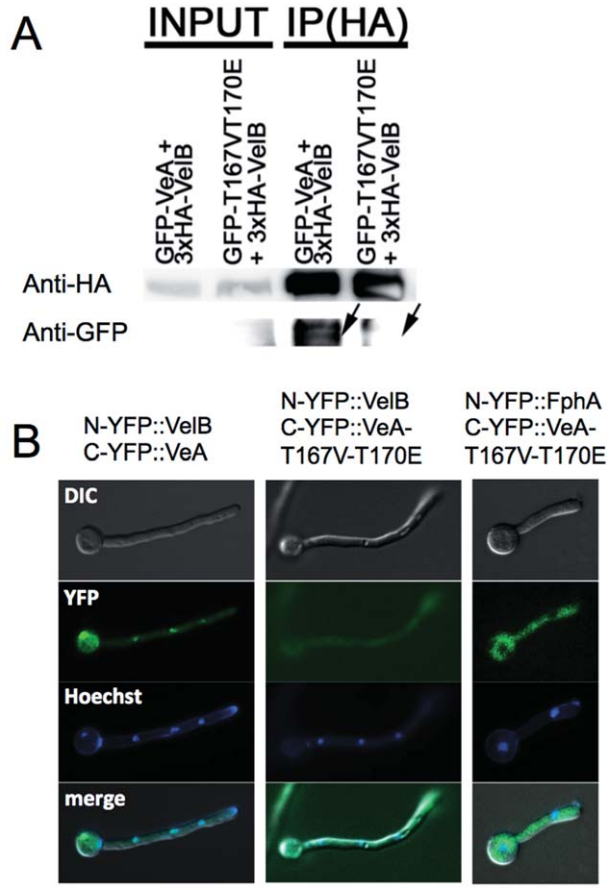

Fig. 6. Interaction of VeA and VelB depends on the phosphorylation status of VeA.
A. CoIP was performed with N-terminal GFP tagged VeA, T167V-T170E mutant and 3×HA-tagged VelB under the inducible *alcA* promoter. Protein purification was performed after 24 h of growth in MM + 2% threonine and 0.2% glucose at 37°C. IP was performed using anti-HA Agarose (Pierce).
B. BiFC of VelB and FphA with VeA and the T167V-T170E mutant. VelB and FphA were fused to the N-terminus of YFP, VeA and the mutant VeA were fused to the C-terminal part. Spores were grown in MM + 2% glycerol and 0.2% glucose (plus markers) and incubated over night at room temperature. Nuclei were stained with Hoechst 33342.

VeA binds its own promoter independently of FphA

We found that different VeA versions apparently lead to different expression levels of *veA* and hypothesized that VeA regulates its own expression by direct promoter binding. Because VeA interacts with FphA, we further hypothesized that FphA and perhaps FphA-dependent VeA phosphorylation could be important for VeA promoter binding. To test the two hypotheses, we performed ChIP experiments. HA-tagged VeA was precipitated and the number of bound *veA*-promoter fragments were quantified by real-time PCR. These experiments revealed indeed binding of VeA independent of the illumination conditions (dark or 15 min white light). Binding was also independent of FphA (Fig. 7). This is in contrast to the regulation of light-regulated genes where VeA–promoter interaction is dependent on FphA (Hedtke *et al*., 2015). Furthermore binding of VelB to the VeA promoter was examined. Although both proteins interact (Fig. 5), VelB is apparently not involved in the binding of VeA to its promoter (Fig. 7).

Discussion

Aspergillus nidulans is a filamentous fungus with a rather versatile lifestyle (Etxebeste *et al*., 2010). It is able to differentiate asexual and sexual spores and can adapt to many different environmental conditions. It is able to use a large number of different carbon, nitrogen and sulfur sources, and produces a great number of secondary metabolites (Yu and Keller, 2005; Yegashi *et al*., 2014). Many of the morphogenetic and metabolic pathways are tightly connected and share some signaling pathways or regulators. One example is the regulation of many processes by light (Bayram *et al*., 2010; Rodriguez-Romero *et al*., 2010). A central component, which is involved in the regulation of many different processes is the global regulator VeA (Calvo, 2008; Bayram and Braus, 2012; Lind *et al*., 2015). VeA belongs to a family of at least four proteins, which share a *velvet* domain with a NF-κB-like DNA-binding motif (Ahmed *et al*., 2013). Thus one regulatory function of VeA is probably direct promoter binding and gene regulation (Kim *et al*., 2009; Lind *et al*., 2015). Likewise, it was shown that VeA controls the expression of

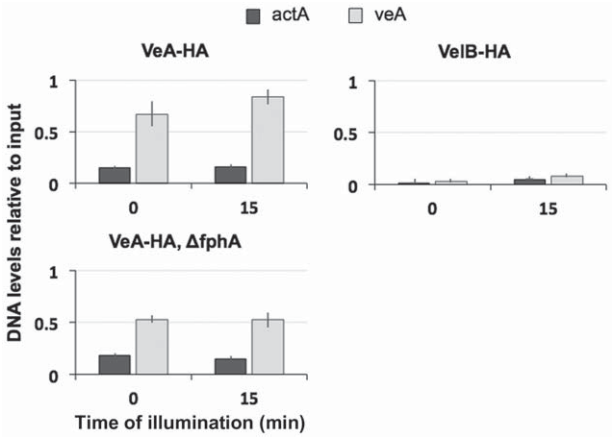

Fig. 7. VeA binds to the own promoter. ChIP of HA-tagged VeA or VelB in darkness and after illumination with white light. Spores were inoculated on plates containing glycerol and incubated in darkness at 37°C. After 3 days, spores were harvested, cross-linked, sonicated and proteins precipitated with anti-HA agarose. DNA was eluted and purified. Quantitative real-time PCR was carried out for the promoters of *veA* and *actA*, which served as a control. DNA levels are relative to input. Error bars represent standard error of the mean.

hundreds of genes (Lind *et al*., 2015). However, the role of VeA appears to be rather complex given that many different pathways are controlled. One important factor in VeA-dependent gene regulation could be its protein concentration. VeA contains a PEST domain, which indicates fast protein turnover. Furthermore, VeA inhibits its own expression and thus a negative feedback loop appears to guarantee appropriate levels of the protein as well. The next level of complexity is at the level of subcellular localization. VeA is abundant in nuclei in the dark, but less abundant in light (Stinnett *et al*., 2007). This implies that pathways, which rely on the DNA-binding activity of VeA will be affected. Last, but not least, there are a number of different protein-interaction partners, each of which probably specific for certain pathways (Bayram *et al*., 2008; Purschwitz *et al*., 2008; Sarikaya-Bayram *et al*., 2015). These interaction partners could be important for DNA binding, but also for subcellular localization, as it was shown for the interaction with LlmF, a protein similar to LaeA (Palmer *et al*., 2013). Here we found that the reversible phosphorylation mimicked using an electric charge at certain amino acids is apparently important for specific functions of the protein. We therefore hypothesize that the phosphorylation status is a key for understanding the complex role of VeA.

There are several lines of evidence that VeA represses asexual development. In a *veA1* mutant, the VeA protein lacks a functional NLS and thus there is less VeA in nuclei. These strains produce more conidia and thus asexual development is stimulated. In contrast, overexpression of *veA* or deletion of the PEST domain inhibit conidiation. The fact that deletion of *veA* does not lead to a large stimulation of conidiation, shows that a cytoplasmic function of VeA is required for efficient conidiation. Change of the phosphorylation status of the four investigated amino acids affected light stimulation, but showed almost no effect in dark samples. The mutant T167E and S183A showed wild type-like conidiation. Therefore, it is most likely that phosphorylation of threonine 167 and dephosphorylation of serine 183 of VeA is required for normal spore production in light and is probably the form found in the cytoplasm.

In comparison with asexual development, sexual development requires VeA in the nucleus. Here, we found that the phosphorylation status causes a delay in the maturation time of cleistothecia in the T167 to valine, T170, S183 and Y254 to glutamic acid and Y254 to phenylalanine mutants. In conclusion, for normal functioning of VeA in the nucleus T167 needs to be phosphorylated, T170, S183 and Y254 need to be dephosphorylated. Surprisingly, the same mutants that were still able to stimulate significant light-dependent conidiation like the wild type were the same with normal cleistothecia maturation. The other way around, mutants with impaired cleistothecia maturation were also less sensitive to light induction. This shows a link of the same phosphorylation status of VeA between asexual and sexual development, although VeA localization plays a different role in both pathways.

It is well known that VeA is required in the nucleus for ST production (Kato *et al*., 2003; Palmer *et al*., 2013). However, little amounts of VeA1 in the nucleus are sufficient to produce more ST in darkness than the wild type. Further overexpression of *veA* also increased ST amounts by twofold. Suggesting that not only the amount of protein is determining ST production as much as the status of the protein. Mimicking different phosphorylation states affected ST biosynthesis. Whereas changes at T167 and 170 showed only minor effects, the mutants S183E and Y254F resulted in a significant increase in ST production. Meaning that phosphorylation at serine 183 and dephosphorylation at tyrosine 254 leads to the induction of ST biosynthesis. In contrast, the S183A mutant showed no effect in dark, but slight induction after illumination. This suggests a major role of S183 in the ST induction process. Tyrosine mutation to glutamic acid showed the same effect as the mutation to phenylalanine and is most likely due to the loss of the aromatic ring and therefore, the results are probably not very meaningful. Still, the significant increase for dephosphorylated Y254 indicates a central role in ST synthesis as well. Considering the localization of S183 and Y254 (Fig. S1), it is likely that a change of the phosphorylation status influences protein interactions, which then leads to a change in ST production. The *ΔPEST* mutant showed, like the *ΔveA* strain, a complete loss of ST production. As the interaction of VeA with LaeA occurs in the C-terminal part of VeA where the PEST domain is located (Bayram *et al*., 2008), it is likely that the interaction with LaeA is impaired and therefore the ST cluster cannot be activated.

The expression of *veA* is inhibited by VeA itself (Kim *et al*., 2009). The *veA1* and the *ΔPEST* mutant show fivefold increased *veA* expression. This can be explained by the fact that in a *veA1* strain, less VeA is localized in the nuclei. The *ΔPEST* variant could be more stable, but should still be localizing like wild-type VeA. Again a loss of interaction with LaeA seems possible as the *veA* expression in *laeA*-deletion strains is increased as well (Bayram *et al*., 2008). Investigation of different phosphorylation status showed strong influence of T167 and T170. We showed that mimicking dephosphorylated T167 and phosphorylated T170 resulted in higher *veA* expression under light conditions whereas dephosphorylated T170 caused an increase in the dark. The opposite effect at T170 suggests a light-dependent pathway that controls *veA*-gene expression. Therefore, in wild type, T170 would be phosphorylated in light and dephosphorylated in the dark to ensure controlled VeA levels. If T167 is dephosphorylated *veA* transcript levels rise after illumination. Both thre-

onines are located in a weak PEST domain in the N-terminal part of VeA and hence might play a role in protein stability.

The analysis of double mutations at T167 and T170 should give insights into additive effects of these phosphorylation sites. Combination of the mutations T167 to V and T170 to E showed a *veA*-deletion-like phenotype at the colony level. This phenotype was only observed in this combination and therefore appears to be highly specific. Expression levels of *veA* under light and dark conditions showed 30- to 60-fold induction respectively in the T167V-T170E mutant compared with wild type. Surprisingly the other combinations showed no increase in *veA* expression although single mutations had an impact. This suggests that two fixed phosphorylation sites counteract the function of VeA single mutations at T167 and T170. From this we conclude that there are different proportions of VeA variants in the cell at certain times. Simultaneous dephosphorylated T167 and phosphorylated T170 therefore cause a loss of VeAs negative feedback on its own expression. Further analysis of the corresponding mutant showed also a lack of sexual development like the *veA*-deletion mutant, but still produced ST like the wild type. In conclusion, T167V-T170E partially phenocopies loss of VeA function.

In order to test whether VeA function in the T167V-T170E mutant is impaired because of changes in the subcellular localization, this VeA variant was visualized and compared with wild-type VeA. In the dark, the T167V-T170E variant showed a comparable behavior as the wild type, but after illumination, still a larger amount of the mCitrine signal was detected in the nuclei. This could mean that the mutants' loss of *veA* transcript inhibition is not due to predominant cytoplasmic localization, but might be caused by the loss of DNA-binding capability or because of the loss of interaction with another protein. VelB would be a likely candidate as *velB* deletion was reported to show comparable phenotypes. Bayram *et al*. (2008) observed that in a *ΔvelB* mutant the *veA* transcript was enriched, there was a loss of sexual development and the ST production was delayed by 24 h. Indeed we were able to show that this interaction is lost in the T167V-T170E mutant. But it still remains unclear if that loss of interaction also results in a loss of DNA-binding activity of the VeA protein. As shown in Fig. 7, VeA binds its own promoter at or near the 'crucial region' (–943 to –740 bp) described in Kim *et al*. 2009, which is involved in the regulation of *veA* expression. And although interaction of VelB and VeA is mostly nuclear, VelB is not directly involved in VeA–DNA binding. To further elucidate how VeA regulates its own expression and how different phosphorylation states influence the binding to the promoter, ChIP experiments with the different phosphorylation mutants are required.

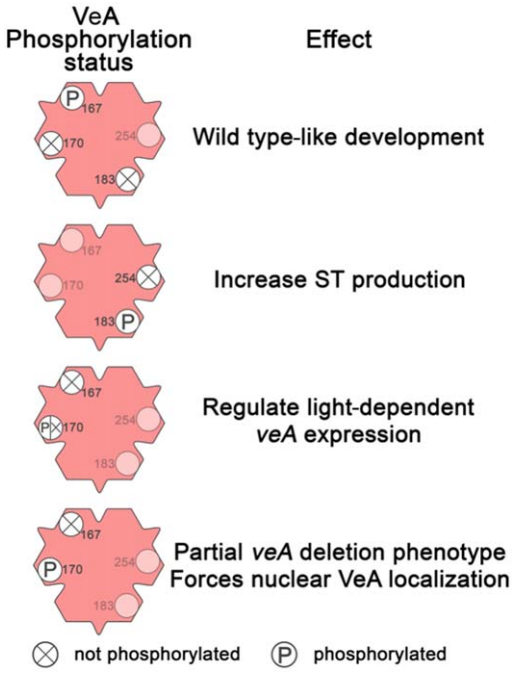

Fig. 8. Schematic illustration of different phosphorylation states of VeA and their physiological roles.

The effects of the phosphorylation status of the four identified amino acids on different pathways, suggests a rather complex regulation. In addition, it has to be made very clear that it is very likely that we were unable to analyze the entire VeA protein with regards to phosphorylation. Hence, it is conceivable that besides the four identified amino acids, other amino acids undergo phosphorylation as well and lead to an even more complicated picture. Here, we propose a model, in which a population of different VeA variants exists in fungal hyphae, and the different variants along with their specific protein interaction partners have different threshold concentrations (Fig. 8). Our analysis paves the way for further experiments to identify kinases and phosphatases that regulate the diverse populations of VeA and maintain the highly sensitive balanced levels of VeA in hyphae. It will be most interesting to decipher the VeA phosphorylation code and see how interacting proteins interpret the phosphorylation status of VeA.

Experimental procedures

Strains and growth conditions

The genotypes of the strains used in this work are given in Table 1. Standard *A. nidulans* molecular and genetic procedures were used (Käfer, 1977). *A. nidulans* transformation was performed as previously described (Yelton *et al*., 1984). Transformation and handling of *Escherichia coli* strains were made through standard procedures (Sambrook and Russel,

Table 1. *Aspergillus nidulans* strains used in this work.

Strain	Genotype	Source
SKV103	*pyrG89, pyroA4, veA+*	Vienken and Fischer, 2006
SKV104	*pabaA1, yA2, pyrG89, pyroA4, veA+*	Kay Vienken
SSR48	*yA2; pyroA4; nku::bar; pabaA1*	This work
SSR56	*yA2; pyroA4; nku::bar; pabaA1; ΔveA::ptrA*	This work
SSR57	*yA2; pyroA4; nku::bar; pabaA1; veA(p)::veA::veA(terminator-120bp)-pyroA4-veA(p)::ptrA*	This work
SSR58	*yA2; pyroA4; nku::bar; pabaA1; veA(p)::veA::veA(terminator-120bp)-pyroA4-veA(p)::ptrA*	This work
SSR60	*yA2; pyroA4; nku::bar; pabaA1; veA(p)::mCitrine::veA-pyroA-veA(p)::ptrA*	This work
SSR67	*yA2; pyroA4; nku::bar; pabaA1; veA(p)::veA-T167E-pyroA-veA(p)::ptrA*	This work
SSR69	*yA2; pyroA4; nku::bar; pabaA1; veA(p)::veA-S183A-pyroA-veA(p)::ptrA*	This work
SSR73	*yA2; pyroA4; nku::bar; pabaA1; veA(p)::veA-T170E-pyroA-veA(p)::ptrA*	This work
SSR74	*yA2; pyroA4; nku::bar; pabaA1; veA(p)::veA-T170V-pyroA-veA(p)::ptrA*	This work
SSR75	*yA2; pyroA4; nku::bar; pabaA1; veA(p)::veA-Y254E-pyroA-veA(p)::ptrA*	This work
SSR79	*yA2; pyroA4; nku::bar; pabaA1; veA(p)::veAΔPEST-pyroA-veA(p)::ptrA*	This work
SSR80	*yA2; pyroA4; nku::bar; pabaA1; veA(p)::veA1-pyroA-veA(p)::ptrA*	This work
SSR86	*yA2; pyroA4; nku::bar; pabaA1; veA(p)::veA-Y254F-pyroA-veA(p)::ptrA*	This work
SSR87	*yA2; pyroA4; nku::bar; pabaA1; veA(p)::veA-T167V-pyroA-veA(p)::ptrA*	This work
SSR88	*yA2; pyroA4; nku::bar; pabaA1; veA(p)::veA-S183E-pyroA-veA(p)::ptrA*	This work
SSR95	*yA2; pyroA4; nku::bar; pabaA1; veA(p)::h2b(p)::veA-pyroA-veA(p)::ptrA*	This work
SSR104	*yA2; pyroA4; nku::bar; pabaA1; veA(p)::veA-T167V/T170V-pyroA-veA(p)::ptrA*	This work
SSR122	*yA2; pyroA4; nku::bar; pabaA1; veA(p)::veA-T167V/T170E-pyroA-veA(p)::ptrA*	This work
SSR137	*yA2; pyroA4; nku::bar; pabaA1; veA(p)::veA/T167E/T170E-pyroA-veA(p)::ptrA*	This work
SSR140	*yA2; pyroA4; nku::bar; pabaA1; veA(p)::veA/T167E/T170V-pyroA-veA(p)::ptrA*	This work
SSR150	*yA2; pyroA4; nku::bar; pabaA1; veA(p)::mCitrine::veA/T167V/T167E-pyroA-veA(p)::ptrA*	This work
SSR151	SKV103 + pMH14: alcA(p)::3xHA::velB, pyroA4, veA+	This work
SSR153	SSR151 + pSR118 + pNZ11: alcA(p)::3xHA::velB, alcA(p)::GFP:veA, pyroA, veA+	This work
SSR154	SSR151 + pSR119 + pNZ11: alcA(p)::3xHA::velB, alcA(p)::GFP::veA-T167V-T170E, pyroA, veA+	This work
SSM12	*yA2; wA3; pyroA4; alcA(p)::3xHA::veA*	Purschwitz *et al*., 2008
SSM50	*alcA::veA::3xHA; pyroA4; ΔfphA::argB*	Hedtke *et al*., 2015
SSM51	*yA2;, arg::trpC; trpC801, ΔveA::argB, alcA(p)::3xHA::VeA*	This work
SSM52	*yA2;, arg::trpC; trpC801, ΔveA::argB, alcA(p)::3xHA::VeAΔPEST*	This work
SMH19	SKV104 + pMH18 (*alcA::n-yfp::velB, pyr4*) + pSR120 (*alcA::c-yfp::veA, pyroA*), *pabaA1*	This work
SMH20	SKV104 + pMH18 (*alcA::n-yfp::velB, pyr4*) + pSR120 (*alcA::c-yfp::veA-T167V-T170E, pyroA*), *pabaA1*	This work
SMH21	SKV103 + pJP4 (*alcA::n-yfp::fphA, pyr4*) + pSR120 (*alcA::c-yfp::veA-T167V-T170E, pyroA*)	

1999). Oligonucleotides used in this work are listed in Table 2 and constructed plasmids in Table 3.

Quantification of asexual and sexual development

From a 10^6 conidia ml^{-1} stock 100 µl were plated in small Petri dishes with MM containing 2% glucose, 1 µg l^{-1} p-aminobenzoic acid and 1 µg l^{-1} pyridoxine. Growth at 37°C for 24 h in darkness was followed by constant illumination for 48 h (asexual) or 96 h (sexual). Controls in constant darkness were incubated for the same time periods. Microscopic pictures were taken after incubation periods (Zeiss: Axio Zoom). For the quantification of conidiospores conidia were washed off the colony surface with a drigalski spatula and 2% Tween20 solution until no conidia were left (10–30 ml per Petri dish). Spore solutions were transferred to a 50 ml falcon tube and filled up to 50 ml. Quantification was done with a Helber counting chamber. To determine the amount of sexual structures a defined area of 4 mm^2 was isolated and cleistothecia as well as primordia were counted.

Phosphatase assay

Protein extracts were prepared as previously described (Purschwitz *et al*., 2008). Each reaction (50 µl) contained 200 µg protein extract and was either treated with or without λ phosphatase (400 U per reaction) from NEB for 1 h at 30°C. Reaction was stopped with 4× SDS loading dye and loaded on a 7.5% SDS polyacrylamide gel. After blotting on a polyvinylidene difluoride membrane, HA-tagged VeA was detected with an anti-HA antibody (Sigma, 1:10.000 dilution).

Analysis of VeA by 2-D gel electrophoresis

Protein extracts from 400 ml liquid culture SSM12 (*alc(A)::3xHA::veA*) grown at 37°C were isolated and HA-VeA purified using the monoclonal antibody HA.11 (dilution 1:200; clone 16B12; Hiss Diagnostics) and protein-G-agarose (Roche). After 1 h of incubation with the HA antibody at 4°C, 50 µl protein-G-agarose was added and incubated for further 3 h at 4°C on a rotator. Centrifugation at 5 rpm for 30 s precipitated HA-VeA, which then was resolved in 2-D-lysis buffer (7 M urea, 2 M thiourea, 2% CHAPS, 0.8% Servalyte3-10, 20 mM Dithiothreitol (DTT)). Samples were mildly shaken for 1 h at 25°C and centrifuged again. The supernatant was used for isoelectric focusing with the Ettan IPGphor II Isoelectric Focusing System (GE Healthcare). IPG strips (Immobiline DryStrip gels, 11 cm, pH 3–11 NL) were rehydrated overnight. Strips were run for 11 h at a gradient from 0 to 1000 V followed by a 2 h gradient from 1000 to 8000 V. Finally, a constant voltage of 8000 V was set until 24 000 V x hrs were achieved. After reduction of proteins with DTT and alkylation with iodine acetamide in equilibration buffer the

Table 2. Oligonucleotides used for real-time PCR, deletion cassettes and molecular cloning.

Name	Sequence (5′-3′)
veAKO LBf	CTCTTCGATGATGACGGCCCTTCG
veAKO LBr	GTTACCAATGGGATCCCGTAATCAATTG CTTGATGGGATAACACAAAATGCTCTAGAAGAC
veAKO RBf	GAAAGACAGTATAATACAAACAAAGATGC TTCTTGGCGGGTTCTGGTATAGGG
veAKO RBr	CGTAATGACTGAACCACCGCTGAC
veAKO nes-f	CGCTCATCGCTGCTCATTGCTG
veAKO nes-r	GTGCTCATTAGGCAAACATTCTGGCTC
veAscr f	CTCGGCTGGAGCATGAGCTG
veAscr r	TCGCGAGTGATCCGGCTGA
veA qRT f	CTCACAGCCGAAACCAATCC
veA qRT r	AAAGTCGTGTCTGCGAACCC
h2B qRT f	TGC CGA GAA GAA GCC TAG CA
h2B qRT r	GAG TAG GTC TCC TTC CTG GT
veA-seq	GGAACGAGGGCTCTTATCGG
T167V f	GGACCCCAAAGACGCAgttGAAGGGACACAGCCCATGCCGTCG
T167V r	CGACGGCATGGGCTGTGTCCCTTCaacTGCGTCTTTGGGGTCC
T170V f	CCCCAAAGACGCAACCGAAGGGgttCAGCCCATGCCGTCGCCCG
T170V r	CGGGCGACGGCATGGGCTGaacCCCTTCGGTTGCGTCTTTGGGG
S183A f	GCCCGTCCCTGGGAAACTGTCGgcACCGCAAGAATTCTTGGAGTTCCGGC
S183A r	GCCGGAACTCCAAGAATTCTTGCGGTgcCGACAGTTTCCCAGGGACGGGC
Y254F f	GGACTACGACTATGATAATGAAAGGGGTttcAACAACCGGCGCCCTGATC
Y254F f	GATCAGGGCGCCGGTTGTTgaaACCCCTTTCATTATCATAGTCGTAGTCC
T167E f	GGACCCCAAAGACGCAgaaGAAGGGACACAGCCCATGCCGTCG
T167E r	CGACGGCATGGGCTGTGTCCCTTCttcTGCGTCTTTGGGGTCC
T170E f	CCCCAAAGACGCAACCGAAGGGgaACAGCCCATGCCGTCGCCCG
T170E r	CGGGCGACGGCATGGGCTGTtcCCCTTCGGTTGCGTCTTTGGGG
S183E f	GCCCGTCCCTGGGAAACTGTCGgaACCGCAAGAATTCTTGGAGTTCCGGC
S183E r	GCCGGAACTCCAAGAATTCTTGCGGTtcCGACAGTTTCCCAGGGACGGGC
Y254E f	GGACTACGACTATGATAATGAAAGGGGTgAaAACAACCGGCGCCCTGATC
Y254E f	GATCAGGGCGCCGGTTGTTTtTcACCCCTTTCATTATCATAGTCGTAGTCC
T167V T170V f	CCC AAA GAC GCA GTC GAA GGG GTA CAG CCC ATG CCG T
T167V T170V r	ACG GCA TGG GCT GTA CCC CTT CGA CTG CGT CTT TGG G
T167E T170V f	CCC AAA GAC GCA GAA GAA GGG GTA CAG CCC ATG CCG T
T167E T170V r	ACG GCA TGG GCT GTA CCC CTT CTT CTG CGT CTT TGG G
T167V T170E f	CCC AAA GAC GCA GAA GAA GGG GAA CAG CCC ATG CCG T
T167V T170E r	ACG GCA TGG GCT GTT CCC CTT CTT CTG CGT CTT TGG G
T167E T170E f	CCC AAA GAC GCA GTC GAA GGG GAA CAG CCC ATG CCG T
T167E T170E r	ACG GCA TGG GCT GTT CCC CTT CGA CTG CGT CTT TGG G
real-actA-fw	CTT CTC AAC ATC CAA CTC CC
real-actA-rv	GGT GGA TTA GAA TCG AAC TAC
real-veA fwd	GGA ATT AGA GAA GCA AGT TGG
real-veA rv	GAT CAC CAA GCT TCA TTA TGG

IPG strips were transferred to the second dimension separation with Criterion Precast Gels (12.5% Tris-HCL, 1.0 mm, IPG + 1 Well Comb, 11 cm from Bio-Rad) fixed with hot agarose solution and subsequently separated for 1 h at 200 V.

Mass spectrometry

Ruthenium stained 2-D gels were used to excise out HA-VeA spots on a Dark Reader Transilluminator (Clare Chemical Research) (Aude-Garcia *et al.*, 2011). Protein spots were destained with ammonium carbonate and acetonitrile. Reduction of disulfide bonds was achieved by treatment with 10 mM DTT in 50 mM ammonium carbonate. Alkylation of free SH was done with 55 mM iodine acetamide in 50 mM ammonium carbonate to stable S-carboxyamidomethylcysteine. In gel trypsin digestion was performed with Sequencing Grade Modified Trypsin (Promega) as described in Shevchenko *et al.* (1996). Peptides were extracted with 50% acetonitirl (v/v) containing 0.1% (v/v) TFA for 10 min by sonication. For mass spectrometry 1 µl of matrix solution (α-cyano-4-hydroxycinnamic acid) was mixed with 1 µl of peptide solution and applied to the anchor-chip target. Mass spectrometry was carried out twice for each sample and isolated VeA peptides

Table 3. Plasmids used in this work.

Plasmids	Construction	Source
pCR2.1-TOPO	Cloning vector	Invitrogen (NV Leek, The Netherlands)
pMCBapx17	For fusion of proteins with GFP under control of *alcA(p)*	V.P. Efimov, Piscataway, New Jersey
pNZ11	pCR2.1-TOPO with pyroA4 marker gene	This work
pMH14	*alcA(p)::3xHA::velB; pyr4*	This work
pMH18	*alcA::N-YFP::velB, pyr4*	This work
pRJ1	*alcA(p)::N-YFP::vipA cloned with Asc*I *and Pac*I, *pyroA, Amp*^{R}	This work
pSM78	*alcA(p)::3xHA::VeA without PEST, pyr4*	This work
pSR08	veA_orf cloned with *Avr*II and *Sal*I in pRJ1, *veA(p)::veA, pyroA*	This work
pSR09	pSR08 with point mutation T167E, *veA(p)::veA-T167E, pyroA*	This work
pSR10	pSR08 with point mutation T170E, *veA(p)::veA-T170E, pyroA*	This work
pSR11	pSR08 with point mutation T170V, *veA(p)::veA-T170V, pyroA*	This work
pSR13	pSR08 with point mutation S183A, *veA(p)::veA-S183A, pyroA*	This work
pSR14	pSR08 with point mutation Y254F, *veA(p)::veA-Y254F, pyroA*	This work
pSR20	pSR08 with point mutation T167V, *veA(p)::veA-T167V, pyroA*	This work
pSR21	pSR08 with point mutation Y254E, *veA(p)::veA-Y254E, pyroA*	This work
pSR35	pSR08 with *Not*I and *Asc*I restriction sites – N-terminally to veA_orf, *veA(p)::veA, pyroA*	This work
pSR36	pSR35 with HA-tag (*Not*I, *Asc*I), *veA(p)::3xHA::veA, pyroA*	This work
pSR41	pSR35 with full-length mCitrine, *veA(p)::mCitrine::veA, pyroA*	This work
pSR51	pSR35 with h2b(p) cloned with *Asc*I and *Not*I; *veA(p)::h2b(p)::veA*	This work
pSR52	pSR08ΔPEST, cloned from pSM78 with *Ssp*I + *Bgl*II, *veA(p)::veAΔPEST*	This work
pSR53	pSR08 with *veA1* mutation; cloned from PCR fragment (863 + 1275) *Mfe*I + *Bam*HI into pSR08, *veA(p)::veA1, pyroA*	This work
pSR63	pSR08 with point mutation S183E, *veA(p)::veA-S183E, pyroA*	This work
pSR70	pSR08 with point mutation T167V and T170V, *veA(p)::veA-T167V-T170V, pyroA*	This work
pSR90	pSR08 with point mutation T167V and T170E, *veA(p)::veA-T167V-T170E, pyroA*	This work
pSR107	pSR41 with point mutation T167V and T170E, *veA(p)::mCitrine::veA-T167V-T170E, pyroA*	This work
pSR108	pSR08 with point mutation T167E and T170E, *veA(p)::veAT167E-T170E, pyroA*	This work
pSR111	pSR08 with point mutation T167E and T170V, *veA(p)::veA-T167E-T170V, pyroA*	This work
pSR118	pMCBapx17 with *veA*, cloned with *Asc*I and *Pac*I, *alcA(p)::GFP::veA, pyrG*	This work
pSR119	pMCBapx17 with *veA-T167V-T170E*, cloned with *Asc*I and *Pac*I, *alcA(p)::GFP::veA-T167V-T170E, pyrG*	This work
pSR120	*alcA::C-YFP::veA, pyroA*	This work
pSR121	*alcA::C-YFP::veA-T167V-T170E, pyroA*	This work
pJP4	*alcA:::n-yfp:::fphA, pyr4*	

were again fragmented. Afterwards tandem mass spectrometry was performed with an Ultraflex I MALDI-TOF/TOF device (Bruker Daltonics) as described in Kniemeyer *et al.* (2006).

Generation of veA *mutants*

To generate mutations of the *veA* gene, the pSR08 plasmid was cloned with 1.5 kb of the *veA* 5′ UTR and 130 bp of the 3′ UTR into the pRJ1 plasmid using *Avr*II and *Sal*I. Site-directed mutagenesis was performed on pSR08 according to the Stratagene QuikChange protocol and the primers listed in Table 2. Mutated plasmids were confirmed via sequencing of the *veA* open reading frame (ORF). The *veA*-deletion strain SSR56 was transformed with different versions of the plasmid pSR08 listed in Table 3. Transformed colonies have been confirmed by PCR and were checked via Southern blot for single and *in locus* integration of the plasmids.

ST isolation and quantification

From a 10^6 conidia ml^{-1} stock 100 µl were plated in small Petri dishes with exactly 10 ml of MM (2% glucose). For each strain and condition, two replicates were grown for 24 h at 37°C in darkness. Subsequent illumination for 48 h with white light (7 J m^{-2}) or continuing incubation in darkness was performed. After incubation, ST was isolated from two disks of agar and mycelia (displaced with the back of a 1 ml tip) by adding 1 ml of chloroform. After vigorously shaking for 30 min at RT, the complete supernatant was dried and resolved in 100 µl acetonitrile. Seven microliters of these extracts were loaded together with 100 µg of a ST standard (Sigma-Aldrich) on silica gels (Macherey-Nagel, silica gel 60, 10 × 20 cm). Resolving buffer was toluol : ethyl-acetate : acetic acid (80:10:10). After running, the silica gel was dried and wetted with saturated $AlCl_3$ solution in 100% EtOH. Consecutive baking for 10 min at 80°C increased the signal intensity, which was photographed after illumination with UV light (365 nm). Quantification was achieved by measuring the band intensity with ImageJ and normalized to the ST standard for each plate.

RNA isolation

Conidia were inoculated with a loop on the surface of 3–8 ml of minimal liquid medium in a Petri dish. After 18 h of incubation in constant darkness at 37°C the mycelial mat was illuminated with white light (0.15 J m^{-2}) LED lamps for 30 min

at 37°C. Control samples were harvested in complete darkness. Samples were frozen in liquid nitrogen and stored at –80°C until RNA isolation. RNA was isolated with the Fungal RNA Extraction kit from Omega according to the RB protocol with minor changes of cell disruption. Cell disruption was performed in a cell homogenizer (Retsch MM200) with glass beads (Qiagen) at 30 hits s^{-1} for 3 min. The isolated RNA was quantified and treated with TURBO DNA-free kit (Ambion). RNA samples were diluted to a final concentration of 50 ng μl^{-1} in DEPC water.

qRT-PCR

Quantitative PCR experiments were performed to determine relative mRNA abundance using SensiFAST SYBR & Fluorescein One-Step Kit from Bioline (Lückenwalde). Each 25 µl reaction contained 0.25 µl of RT enzyme (Bioline), 0.2 µM of primers (salt free grade) and 100 ng of total RNA. The cycle included 10 min at 45°C for the reverse transcription reaction, followed 150 s at 95°C for its inactivation and 40 PCR cycles (10 s at 95°C, and 30 s at 55°C). After each PCR, we performed melting curve analyses (80 cycles, 95°C to 55°C with 10 s per step) to show the specific amplification of single DNA segments and the absence of non-specifically amplified DNA.

The results for each gene were normalized to the corresponding results obtained with *h2B* to correct for sampling errors. Then, the results obtained for each sample were in most cases normalized to the RNA sample obtained from wild-type mycelia in darkness or exposed to light for 30 min and are the average of three to six biological replicates. For oligonucleotides, Chromatin-Immunoprecipiatation (ChIP) was performed as described (Hedtke *et al*., 2015) see Table 2.

Fluorescence microscopy

For the localization studies we used an AxioImager Z.1 from Zeiss operated with the ZEN software. Pictures were recorded with an AxioCam MR camera and a 63X Plan-ApoChromat lens. VeA protein was fused to mCitrine N-terminally from mCitrine LIC cloning vector (u-mCitrine) pET. The plasmid was a gift from Scott Gradia (Addgene plasmid # 29771). Expression was performed under the natural promoter and *in locus* recombination. Samples were inoculated on cover slips with MM (2% glucose) for 16 h at 30°C and either kept in darkness or illuminated (7 J m^{-2}). Mycelia were fixed by treatment with 1 × PBS with 4% paraformaldehyde for 15 min at RT. Subsequent washing with 1 × PBS was performed. Addition of 1 µl of DAPI (VECTASHIELD®) just before analyzing the samples allowed investigation of nuclear localization.

For BiFC, spores were inoculated on cover slips in liquid minimal medium containing 2% glycerol and 0.2% glucose (and necessary markers) and were incubated over night at RT. The next day, cover slips were mounted on microscope slides and hyphae were examined under the microscope. VelB and FphA were fused to the N-terminal part of YFP; VeA and the T167VT170E mutant were fused to the C-terminal part of YFP under the inducible *alcA* promoter. Hoechst 33342 was used for nuclear staining.

Quantification of fluorescence signal in the nucleus

To quantify the amount of VeA signal in the nucleus, we measured the fluorescence pixel counts with the plugin color pixel counter for ImageJ. We determined total hyphal fluorescence counts and nuclei-specific counts by measurement of DAPI-stained areas of the hyphae. A minimum of six microscopic pictures has been evaluated.

Co-immunoprecipitation

Co-immunoprecipitation was performed as described earlier in Hedtke *et al*. (2015). For the investigation of protein interactions, the strains SSR153 and SSR154 were used.

Acknowledgements

This work was supported by the German Science Foundation (DFG). We thank Scott Gradia (University of California, Berkley, CA, USA) for the kind gift of the mCitrine vector. We thank Birgit Schreckenberger for technical assistance.

References

Adams, T.H., Wieser, J.K., and Yu, J.-H. (1998) Asexual sporulation in *Aspergillus nidulans*. *Microbiol Mol Biol Rev* **62:** 35–54.

Ahmed, Y.L., Gerke, J., Park, H.S., Bayram, O., Neumann, P., Ni, M., *et al*. (2013) The velvet family of fungal regulators contains a DNA-binding domain structurally similar to NF-kappaB. *PLoS Biol* **11:** e1001750.

Amaike, J., and Keller, N.P. (2009) Distinct roles for VeA and LaeA in development and pathogenesis of *Aspergillus flavus*. *Eukaryot Cell* **8:** 1051–1060.

Anrather, J., Racchumi, G., and Iadecola, C. (2005) cis-Acting, element-specific transcriptional activity of differentially phosphorylated nuclear factor-kappa B. *J Biol Chem* **280:** 244–252.

Aude-Garcia, C., Collin-Faure, V., Luche, S., and Rabilloud, T. (2011) Improvements and simplifications in in-gel fluorescent detection of proteins using ruthenium II tris-(bathophenanthroline disulfonate): the poor man's fluorescent detection method. *Proteomics* **11:** 324–328.

Bayram, O., Krappmann, S., Ni, M., Bok, J.W., Helmstaedt, K., Valerius, O., *et al*. (2008) VelB/VeA/LaeA complex coordinates light signal with fungal development and secondary metabolism. *Science* **320:** 1504–1506.

Bayram, Ö., and Braus, G.H. (2012) Coordination of secondary metabolism and development in fungi: the velvet family of regulatory proteins. *FEMS Microbiol Rev* **36:** 1–24.

Bayram, Ö., Braus, G.H., Fischer, R., and Rodriguez-Romero, J. (2010) Spotlight on *Aspergillus nidulans* photosensory systems. *Fungal Genet Biol* **47:** 900–908.

Bayram, Ö., Bayram, Ö.S., Ahmed, Y.L., Maruyama, J., Valerius, O., Rizzoli, S.O., *et al*. (2012) The *Aspergillus nidulans* MAPK moduld AnSte11-Ste50-Ste7-Fus3 controls development and secondary metabolism. *PLoS Genet* **8:** e1002816.

Beyhan, S., Gutierrez, M., Voorhies, M., and Sil, A. (2013) A temperature-responsive network links cell shape and viru-

lence traits in a primary fungal pathogen. *PLoS Genet* **8:** e1002816.
Blumenstein, A., Vienken, K., Tasler, R., Purschwitz, J., Veith, D., Frankenberg-Dinkel, N., and Fischer, R. (2005) The *Aspergillus nidulans* phytochrome FphA represses sexual development in red light. *Curr Biol* **15:** 1833–1838.
Bok, J.W., Soukup, A.A., Chadwick, E., Chiang, Y.M., Wang, C.C., and Keller, N.P. (2013) VeA and MvlA repression of the cryptic orsellinic acid gene cluster in *Aspergillus nidulans* involves histone 3 acetylation. *Mol Microbiol* **89:** 963–974.
Brandt, S., von Stetten, D., Günther, M., Hildebrandt, P., and Frankenberg-Dinkel, N. (2008) The fungal phytochrome FphA from *Aspergillus nidulans*. *J Biol Chem* **283:** 34605–34614.
Calvo, A.M. (2008) The VeA regulatory system and its role in morphological and chemical development in fungi. *Fungal Genet Biol* **45:** 1053–1061.
Calvo, A.M., and Cary, J.W. (2015) Association of fungal secondary metabolism and sclerotial biology. *Front Microbiol* **6:** 62.
Calvo, A.M., Bok, J.W., Brooks, W., and Keller, N.P. (2004) *veA* is required for toxin and sclerotial production in *Aspergillus parasiticus*. *Appl Environ Microbiol* **70:** 4733–4939.
Clutterbuck, A.J. (1977) The genetics of conidiation in *Aspergillus nidulans*. In *Genetics and Physiology of* Aspergillus. Smith, J.E., and Pateman, J.A. (eds). London: Academic Press, pp. 305–318.
Dhingra, S., Andes, D., and Calvo, A.M. (2012) VeA regulates conidiation, gliotoxin production, and protease activity in the opportunistic human pathogen *Aspergillus fumigatus*. *Eukaryot Cell* **11:** 1531–1543.
Dreyer, J., Eichhorn, H., Friedlin, E., Kürnsteiner, H., and Kück, U. (2007) A homologue of the Aspergillus vevet gene regulates both cephalosporin C biosynthesis and hyphal fragmentation in *Acremonium chrysogenum*. *Appl Environ Microbiol* **73:** 3412–3422.
Duran, R.M., Cary, J.W., and Calvo, A.M. (2007) Production of cyclopiazonic acid, aflatrem, and aflatoxin by *Aspergillus flavus* is regulated by *veA*, a gene necessary for sclerotial formation. *Appl Microbiol Biotechnol* **73:** 1158–1168.
Etxebeste, O., Garzia, A., Espeso, E.A., and Ugalde, U. (2010) *Aspergillus nidulans* asexual development: making the most of cellular modules. *Trends Microbiol* **18:** 569–576.
Hedtke, M., Rauscher, S., Röhrig, J., Rodriguez-Romvero, J., Yu, Z., and Fischer, R. (2015) Light-dependent gene activation in *Aspergillus nidulans* is strictly dependent on phytochrome and involves the interplay of phytochrome and white collar-regulated histone H3 acetylation. *Mol Microbiol* **97:** 733–745.
Hoff, B., Kamerewerd, J., Sigl, C., Mitterbauer, R., Zadra, I., Kürnsteiner, H., and Kück, U. (2010) Two components of a velvet-like complex control hyphal morphogenesis, conidiophore develoment, and penicillin biosynthesis in *Penicillium chrysogenum*. *Eukaryot Cell* **9:** 1236–1250.
Jun, S.C., Lee, S.J., Park, H.J., Kang, J.Y., Leem, Y.E., Yang, T.H., *et al*. (2011) The MpkB MAP kinase plays a role in post-karyogamy processes as well as in hyphal anastomosis during sexual development in *Aspergillus nidulans*. *J Microbiol* **49:** 418–430.
Karakkat, B.B., Gold, S.E., and Covert, S.F. (2013) Two members of the *Ustilago maydis* velvet family influence teliospore development and virulence on maize seedlings. *Fungal Genet Biol* **61:** 111–119.
Kato, N., Brooks, W., and Calvo, A.M. (2003) The expression of sterigmatocystin and penicillin genes in *Aspergillus nidulans* is controlled by *veA*, a gene required for sexual development. *Eukaryot Cell* **2:** 1178–1186.
Käfer, E. (1965) The origin of translocations in *Aspergillus nidulans*. *Genetics* **52:** 217–232.
Käfer, E. (1977) Meiotic and mitotic recombination in *Aspergillus* and its chromosomal aberrations. *Adv Genet* **19:** 33–131.
Kim, H.-J., Han, J.-H., Kim, K.S., and Lee, Y.-H. (2014) Comparative functional analysis of the velvet gene family reveals unique roles in fungal development and pathogenicity in *Magnaporthe oryzae*. *Fungal Genet Biol* **66:** 33–43.
Kim, H.-S., Han, K.-Y., Kim, K.-J., Han, D.-M., Jahng, K.-Y., and Chae, K.-S. (2002) The *veA* gene activates sexual development in *Aspergillus nidulans*. *Fungal Genet Biol* **37:** 72–80.
Kim, H.-Y., Han, K.-H., Lee, M.-H., Oh, M., Kim, H.-S., Zhixiong, X., *et al*. (2009) The veA gene is necessary for the negative regulation of the veA expression in *Aspergillus nidulans*. *Curr Genet* **55:** 391–397.
Kniemeyer, O., Lessing, F., Scheibner, O., Hertweck, C., and Brakhage, A.A. (2006) Optimisation of a 2-D gel electrophoresis protocol for the human-pathogenic fungus Aspergillus fumigatus. *Curr Genet* **49:** 178–189.
Li, S., Myung, K., Guse, D., Donkin, B., Proctor, R.H., Grayburn, W.S., and Calvo, A.M. (2006) FvVE1 regulates filamentous growth, the ratio of microconidia to macroconidia and cell wall formation in *Fusarium verticillioides*. *Mol Microbiol* **62:** 1418–1432.
Lind, A.L., Wisecaver, J.H., Smith, T.D., Feng, X., Calvo, A.M., and Rokas, A. (2015) Examining the evolution of the regulatory circuit controlling secondary metabolism and development in the fungal genus *Aspergillus*. *PLoS Genet* **11:** e1005096.
Myung, K., Li, S., Butchko, R.A.E., Busman, M., Proctor, R.H., Abbas, H.K., and Calvo, A.M. (2009) FvVE1 regulates biosynthesis of the mycotoxins fumonisins and fusarins in *Fusarium verticillioides*. *J Agric Food Chem* **57:** 255–259.
Palmer, J.M., Theisen, J.M., Duran, R.M., Grayburn, W.S., Calvo, A.M., and Keller, N.P. (2013) Seconary metabolism and development is mediated by LlmF control of VeA subcellular localization in *Aspergillus nidulans*. *PLoS Genet* **9:** e1003193.
Park, H.S., Ni, M., Jeong, K.C., Kim, Y.H., and Yu, J.H. (2012) The role, interaction and regulation of the velvet regulator VelB in *Aspergillus nidulans*. *PLoS ONE* **7:** e45935.
Park, H.S., Nam, T.Y., Han, K.H., Kim, S.C., and Yu, J.H. (2014) VelC positively controls sexual development in *Aspergillus nidulans*. *PLoS ONE* **9:** e89883.
Purschwitz, J., Müller, S., Kastner, C., Schöser, M., Haas, H., Espeso, E.A., *et al*. (2008) Functional and physical interaction of blue and red-light sensors in *Aspergillus nidulans*. *Curr Biol* **18:** 255–259.
Purschwitz, J., Müller, S., and Fischer, R. (2009) Mapping the interaction sites of *Aspergillus nidulans* phytochrome FphA

with the global regulator VeA and the white collar protein LreB. *Mol Genet Genomics* **281:** 35–42.
Rechsteiner, M. (1990) PEST sequences are signals for rapid intracellular proteolysis. *Semin Cell Biol* **1:** 433–440.
Rechsteiner, M., and Rogers, S.W. (1996) PEST sequences and regulation by proteolysis. *Trends Biochem Sci* **21:** 267–271.
Rodriguez-Romero, J., Hedtke, M., Kastner, C., Müller, S., and Fischer, R. (2010) Fungi, hidden in soil or up in the air: light makes a difference. *Annu Rev Microbiol* **64:** 585–610.
Sambrook, J., and Russel, D.W. (1999) *Molecular Cloning: A Laboratory Manual*. Cold Spring Harbor, NY: Cold Spring Harbor Laboratory Press.
Sarikaya-Bayram, O., Bayram, Ö., Feussner, K., Kim, J.-H., Kim, H.-S., Kaever, A., *et al*. (2014) Membrane-bound methyltransferase complex VapA–VipC–VapB guides epigenetic control of fungal development. *Dev Cell* **29:** 406–420.
Sarikaya-Bayram, O., Palmer, J.M., Keller, N., Braus, G.H., and Bayram, Ö. (2015) One Juliet and four Romeos: VeA and its methyltransferases. *Front Microbiol* **6:** 1.
Schumacher, J., Simon, A., Cohrs, K.C., Traeger, S., Porquier, A., Dalmais, B., *et al*. (2015) The VELVET complex in the gray mold fungus *Botrytis cinerea*: impact of BcLAE1 on differentiation, secondary metabolism and virulence. *Mol Plant Microbe Interact* **28:** 659–674.
Shevchenko, A., Jensen, O.N., Podtelejnikov, A.V., Sagliocco, F., Wilm, M., Vorm, O., Mortensen, P., Boucherie, H., and Mann, M. (1996) Linking genome and proteome by mass spectrometry: large-scale identification of yeast proteins from two dimensional gels. *Proc Natl Acad Sci U S A* **93:** 14440–14445.
Stinnett, S.M., Espeso, E.A., Cobeno, L., Araujo-Bazan, L., and Calvo, A.M. (2007) *Aspergillus nidulans* VeA subcellular localization is dependent on the importin alpha carrier and on light. *Mol Microbiol* **63:** 242–255.
Timberlake, W.E. (1990) Molecular genetics of *Aspergillus* development. *Annu Rev Genet* **24:** 5–36.
Vienken, K., and Fischer, R. (2006) The $Zn(II)_2Cys_6$ putative transcription factor NosA controls fruiting body formation in *Aspergillus nidulans*. *Mol Microbiol* **61:** 544–554.
Wang, F., Djiksterhuis, J., Wyatt, T., Wösten, H.A.B., and Bleichrodt, R.-J. (2015) VeA of *Aspergillus niger* increases spore dispersing capacity by impacting conidiophore architecture. *Antonie Van Leeuwenhoek* **107:** 187–199.
Webster, R.H., and Sil, A. (2008) Conserved factors Ryp2 and Ryp3 control cell morphology and infectious spore formation in the fungal pathogen *Histoplasma capsulatum*. *Proc Natl Acad Sci USA* **105:** 14573–14578.
Wiemann, P., Broiwn, D.W., Kleigrewe, K., Bok, J.W., Keller, N.P., Humpf, H.-U., and Tudzynski, B. (2010) FfVel1 and FfLae1, components of a velvet-like complex in *Fusarium fujikuroi*, affect differentiation, secondary metabolism and virulence. *Mol Microbiol* **77:** 972–994.
Yegashi, J., Oakley, B.R., and Wang, C.C. (2014) Recent advances in genome mining of secondary metabolite biosynthetic gene clusters and the development of heterologous expression systems in *Aspergillus nidulans*. *J Ind Microbiol Biotechnol* **41:** 433–442.
Yelton, M.M., Hamer, J.E., and Timberlake, W.E. (1984) Transformation of *Aspergillus nidulans* by using a *trpC* plasmid. *Proc Natl Acad Sci USA* **81:** 1470–1474.
Yu, J.H., and Keller, N. (2005) Regulation of secondary metabolism in filamentous fungi. *Annu Rev Phytopathol* **43:** 437–458.

Supporting information

Additional supporting information may be found in the online version of this article at the publisher's web-site.